RESEARCHES CONCERNING NUTS DEFORMATION IN THE CASE OF THREADED ASSEMBLY

CRISTEA ION

Universty of Bacau

Abstract: Nut deformation, which is the main cause of the tightening characteristics loss in a threaded assembly, was analytical and experimental analyzed. A method for the analysis of nut radial deformation was proposed. The performed experiments confirmed the validity of this method and the main conclusion of this paper is that the tightening stress generates a contraction radial deformation on the nut frontal surface, which leads to the increasing of the assembly strength.

1. Introduction

Many years it was considering that the diminishing of the threaded assemblies is due to the elasto-plastic deformations of the nut and screw threads. Different studies were performed in this sense but their principal goal was to estimate the assembly elasticity constant in the case of compression or pulsatory loading. The method proposed in this work allows the analysis of radial deformations of three types of nuts and the performed experiments confirm the method validity.

2. Theoretical analysis

It is considered that the forces equilibrium from fig. 1,a was replaced with an axial force q(z) and a radial one p(z), which act on the inner surface of nut as in fig. 1,b and fig. 1,c. The relation between q(z) and p(z) could be obtained from the equilibrium of forces which act on the thread flanks as in fig. 2,a, resulting:

$$p(z)/q(z) = tan(\alpha-\rho)$$

where: α is half of the thread angle and ρ is the friction angle.

$$P(z) = Fnsin\alpha - Fncos\alpha$$
, $q(z) = Fnsin\alpha + Fncos\alpha$, $\mu_s = tan\rho$.

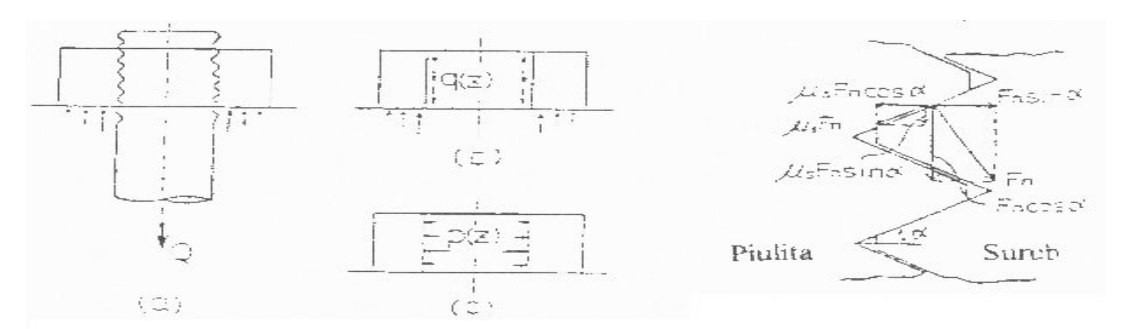


Fig. 1 Forces equilibrium

Fig.2 Ratio p(z)/q(z) on the thread surface

In fig. 3 a simplified model of nut with inner diameter 2a, external diameter 2b and height h is presented.

$$\sigma_{r} = \frac{\partial}{\partial z} \left(\upsilon \Delta^{2} \Phi - \frac{\partial^{2} \varphi}{\partial r^{2}} \right)$$

$$\sigma_{\theta} = \frac{\partial}{\partial z} \left(\upsilon \Delta^{2} \Phi - \frac{\partial^{2} \varphi}{\partial r^{2}} \right)$$

$$\sigma_{z} = \frac{\partial}{\partial z} \left[(2 - \upsilon) \Delta^{2} \Phi - \frac{\partial^{2} \varphi}{\partial z^{2}} \right]$$

$$\tau_{rz} = \frac{\partial}{\partial \tau} \left[(1 - \upsilon) \Delta^{2} \Phi - \frac{\partial^{2} \varphi}{\partial z^{2}} \right]$$
(2)

Fig. 3 Coordinate system of nut

v – Poisson's coefficient

When on the inner surface of thread act the symmetric axial forces q(z) and p(z), the function Φ is [3]:

$$\Phi = \sum_{n=1;2...} \sin \beta_n z \{ a_n I_0(\beta_n r) + b_n \beta_n r I_1(\beta_n r) + a'_n K_0(\beta_n r) + b'_n \beta_n K_1(\beta_n r) \} +$$

$$+ \sum_{n=1;2} \cos \beta_n z \{ c_n I_0(\beta_n r) + d_n \beta_n r I_1(\beta_n r) + c'_n K_0(\beta_n r) + d'_n \beta_n r K_1(\beta_n r) \}$$
(3)

where $\beta_n = (2n-1)\pi/2h$, $I_0(\beta_n r)$, $I_1(\beta_n r)K_0(\beta_n r)$ are the first two Bassel functions of order zero and one and $a_n \dots d_n$ are undetermined coefficients. By replacing equation 3 in equation 2 results:

$$\sigma_{r} = \sum -\beta_{n}^{3} \cos \beta_{n} z \left\{ a_{n} \left[I_{0}(\beta_{n}r) - \frac{I_{1}(\beta_{n}r)}{\beta_{n}r} \right] + b_{n} \left[(1 - 2\gamma)I_{0}(\beta_{n}r) + \beta_{n}rI_{1}(\beta_{n}r) \right] + \right\}$$

$$+ a'_{n} \left[K_{0}(\beta_{n}r) + \frac{K_{1}(\beta_{n}r)}{\beta_{n}r} \right] + b'_{n} \left[-(1 - 2\nu)K_{0}(\beta_{n}r) + \beta_{n}rK_{1}(\beta_{n}r) \right] +$$

$$+ \sum \beta_{n}^{3} \sin \beta_{n} z \left\{ c_{n} \left[I_{0}(\beta_{n}r) - \frac{I_{1}(\beta_{n}r)}{\beta_{n}r} \right] + d_{n} \left[(1 - 2\nu)I_{0}(\beta_{n}r) + \beta_{n}rI_{1}(\beta_{n}r) \right] +$$

$$+ c'_{n} \left[K_{0}(\beta_{n}r) + \frac{K_{1}(\beta_{n}r)}{\beta_{n}r} \right] + d'_{n} \left[(1 - 2\nu)K_{0}(\beta_{n}r) + \beta_{n}rK_{1}(\beta_{n}r) \right] \right\}$$

$$(4)$$

In this paper, the undetermined coefficients are chosen by points method in order to satisfy the boundary condition expressed by equation 5:

(5)

- (I) A_t r=a: $\tau_{1,2}$ =q(z), σ_r =-p(z), -p(z)/q(z) = -tan (α -p) (II) A_t r=b: $\tau_{1,2}$ =0, σ_t =0,
- (III) $A_t = 0: \tau_{1,2} = \tau_{rz}(r), \sigma_z = \sigma_{z(t)}(r),$
- (IV) $A_t = h: \tau_{1,2} = 0, \sigma_z = 0,$

Where q(z) and p(z) show the load distribution on the thread flanks. The relation between q(z) and the axial force Q is: $Q = 2\pi a q(z) dz$ $\sigma_z(r)$ for z = 0, under the boundary condition given by equation 5.

The pressure τ_{rzo} (r) is equivalent with the friction force and could be obtained as follows: firstly, the σ_{zo} (r) distribution is obtained in absence of friction and τ_{rzo} (r) is recalculated with equation $\tau_{rz}(r) = \mu_w(r) \ \sigma_{z0}(r)$ where μ_w (r) is the friction coefficient obtained from the equation τ_{rz0} (r), where μ_w is the maximum value of the friction coefficient. In the absence of friction, the boundary condition given by the eq. 5 for $\mu_s = \mu_w = 0$ could be written: $-p(z)/q(z) = -\tan\alpha$ end τ_{rz0} (r) = 0 for z=0.

The function Φ from eq. 3 consists of a finite number of terms (n = 6) and 48 point on lines, chosen such that the coefficients $a_n \dots a_n$ (n = 1, 2, ...6) could be determined. If the boundary condition from eq. 5 is satisfied, 48 equations with 48 unknowns are obtained. The undetermined coefficients could be obtained from the equations solutions, and the pressure components result from eq. 4. The radial deformations U of nut could be obtained by introducing the pressure components into eq. 6, where E is the Young's modulus of the nut material.

$$u = \frac{r}{E} \left[\sigma_e - \upsilon \left(\sigma_r + \sigma_z \right) \right] \tag{6}$$

3. Numerical calculus and discussions

Three nuts M 18x2,5 of different types were deformed; the normal nut (A), the nut with the increased diameter (B) and the tall nut (C), fig. 4. the main characteristics of these nut are given in table 1.

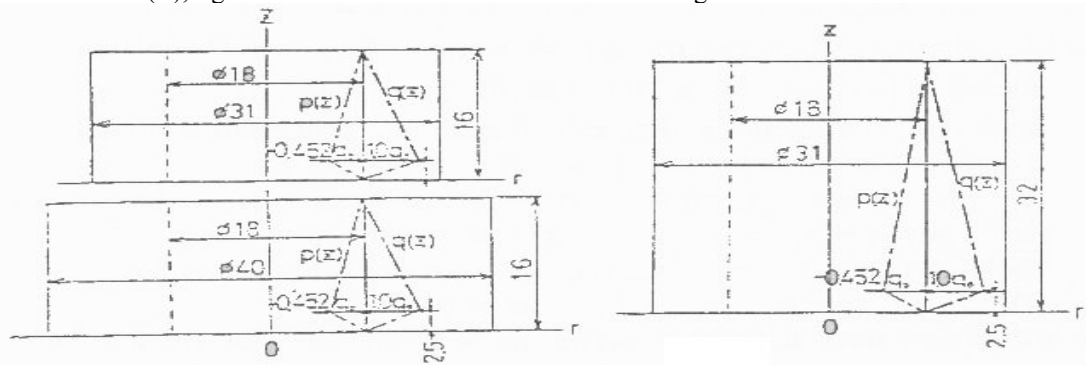


Fig. 4. Example of numerical calculus

For the calculus of the nuts deformations, n=5 terms were taken in eq. 3 and m=48 points. Positions of these points were chosen at the equal distances from the nut edge. In the calculus results, the values σ_r/q_0 and τ_{rz}/q_0 at the middle points approximate the demanded value $\sigma_r/q_0 = \tau_{rz}/q_0 = 0$ because the values are smaller than $,45x10^-$ 2. Besides, on the inner surface could be seen (fig. 5) that the calculated (plane curves lines) $\sigma_r(z)$ and $\tau_{r2}(z)$ are fitted very well with theoretical q(z) and p(z) from the dash doted lines.

Characteristics nut	Inner diameter 2a [mm]	External diameter 2b [mm]	Young's modulus E [GPa]	Height h [mm]	Poisson's coefficient
(A) normal nut	18.0	31	206	16	0.3
(B) nut with the increased external diameter	18.0	41	206	16	0.3
(C) tall nut	18.0	31	206	16	0.3

On fig. 6 the radial deformations of the internal and external surfaces of nut are shown. From the figure results that the frontal surfaces and the strength surface of nut increase in radial direction under p(z) action while the

end decreases and the strength surface increases under q(z) action. Thus, the nut obeys to contractions on the radial direction to the frontal surfaces and to increasing of the strength surface due to the deformations overlap. In order to verify experimentally the obtained results, two nuts were tested to traction, on a traction testing universal machine. The radial deformations were determined by using an electronic micrometer. In fig. 7 the comparative analysis between the experimental and calculated results for the radial deformations of the external surface of nut is presented. It could be observed that all calculated elements coincide with the experimental ones, excepting the tall nut for which a uniform distribution of load in screw-nut assembly it was considered.

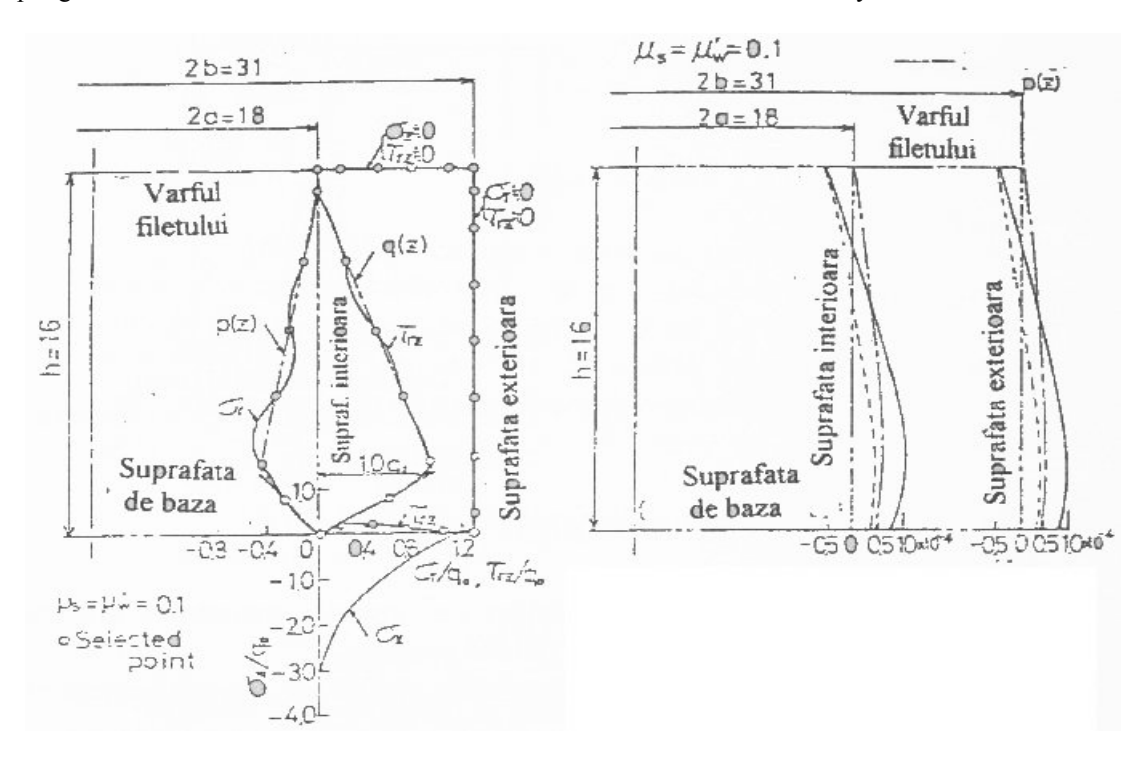


Fig. 5 Pressure distribution on the boundary surfaces of the thread

$$\begin{aligned} \text{Axial tension } Q &= 27kN \\ \text{Nut 1} \\ \text{Nut 2} \\ \text{Calculated values} \\ &\underline{\qquad} \quad \mu_s = \mu_w = 0,1 \\ ------ \quad \mu_s &= \mu_w = 0 \end{aligned}$$

Fig. 7 Comparative analysis of the results

20=18 (Ton icce) (Secring surface) (Secring surface)

Fig.6

4. Conclusions

In order to analyze the nut deformation, a method which divides the action force into two components (radial and axial) was proposed.

The calculated values for the radial deformations of nut coincide with the experimental ones. It is evident that the nut deformation is due to the overlap of two deformations: radial and axial, respectively.

5. References

- [1] Chisiu, A., Machines organs, E. T., Bucharest, 1976, p.129
 [2] Hongou, K, Mechanical Engineering, 1964, p.30, 215,434
 [3] Timoshenko, Goodier, J.N., Theory of elasticity, McGraw-Hill, New York, 1970, p.424